Nucleic Acids Research, 1997, Vol. 25, No. 14 **2835–2840**

Determinants of a protein-induced RNA switch in the large domain of signal recognition particle identified by systematic-site directed mutagenesis

Krishne Gowda and Christian Zwieb*

Department of Molecular Biology, The University of Texas Health Science Center at Tyler, Highway 271 N, PO Box 2003, Tyler, TX 75710, USA

Received March 27, 1997; Revised and Accepted June 4, 1997

ABSTRACT

Signal recognition particle (SRP) is a ribonucleoprotein complex that associates with ribosomes to promote the co-translational translocation of proteins across biological membranes. Human SRP RNA molecules exist in two distinct conformations, SR-A and SR-B, which may exchange during the assembly of the particle or could play a functional role in the SRP cycle. We have used systematic site-directed mutagenesis of the SRP RNA to determine the electrophoretic mobilities of altered RNA molecules, and we have identified the nucleotides that avert the formation of the two conformers. The conformer behavior of the various RNAs was addressed quantitatively by calculating a value ζ as an indicator of conformational variability. Single loose A-like forms were induced by changes in helix 5 [nucleotides (nt) at positions 111–128 or 222–231], helix 6 (nt at positions 141–150) and helix 7 (nt at position 169 and 170), whereas other mutations in helix 6 and helix 8 preserved the conformational variability of the mutant RNA molecules. The more compact B-like form was induced only when a small region (129-CAAUAU-134), located in the 5′-proximal portion of helix 6, was altered. Since this region is part of the binding site for SRP19, we suggest that protein SRP19 uses nucleotides at 129–134 to trigger the formation of the favored SR-B-form, and thus directs an early step in the hierarchical assembly of the large SRP domain.

INTRODUCTION

Conformational differences in RNA molecules reflect their functional importance in a wide variety of cellular processes (1–3). Because of its small size, signal recognition particle (SRP), a cytosolic ribonucleoprotein complex involved in the translation of secretory proteins and their translocation across lipid bilayers (reviewed in 4), serves as a convenient model system for resolving molecular details of how conformational switching can occur in the RNA. The SRP has been characterized best in the mammalian system where it is an elongated particle with a small and a large domain separated by a variable adapter region (5,6). Chemical and enzymatic modification experiments, electron microscopy, comparative sequence analysis and model building were among the methods used to determine the structural and functional properties of the SRP components (5–11).

SRP contains six proteins, of which SRP9, SRP14, SRP19, SRP54 and SRP68, are in direct contact with the SRP RNA (10,12). Of special interest is protein SRP54 as it requires SRP19 for assembly. Since no interactions between the free SRP19 and SRP54 proteins were detected, a conformational change in the large domain of the SRP RNA was postulated to accompany the sequential binding of these two polypeptides (13,14).

Experimental support for conformational changes was provided by the discovery of two distinct major SRP RNA forms, SR-A and SR-B, on non-denaturing polyacrylamide gels (15,16). The faster-migrating B-form was preferred by protein SRP19 over the slow-migrating A-form, and association of SRP19 with SRP RNA resulted in the reconstitution of a uniform complex (17). However, the location of the SRP RNA switch remained unknown. Furthermore, the role of protein SRP19 in the triggering of the RNA switch was unresolved.

The detailed molecular analysis of RNA switches is hampered by the fact that they tend to form the core of a folded RNA molecule. This is in contrast to the analysis of RNA–protein interactions where nucleotides may be accessible on the surface and therefore are amenable to enzymatic and chemical modifications. Therefore, to identify the sites in SRP RNA that influence conformation, we chose a systematic site-directed mutagenesis approach for introducing changes throughout the large domain of the human SRP RNA (18) as this approach had the advantage that all sites could be analyzed, including those that were hidden from external probes. Introducing mutations systematically assured that the results were unbiased towards the functional role of a particular site. A small region was identified in the SRP RNA that triggers the formation of SR-B. This trigger sequence may be used by protein SRP19 to induce the preferred B-conformer.

MATERIALS AND METHODS

Construction and synthesis of mutant SRP RNAs

Plasmids coding for authentic human SRP RNA or for mutant RNAs that lacked individual RNA helices were described earlier (14). Mutant ΔH67 was generated by PCR site-directed mutagenesis (19) using oligonucleotide 5′-CGGTTCACCCCTTGCCGAACTTAGTG-3′ as a mutagenic primer. Details of the construction of other mutations in the large domain of the SRP were communi-

*To whom correspondence should be addressed. Tel: +1 903 877 7689; Fax: +1 903 877 5731; Email: zwieb@uthct.edu

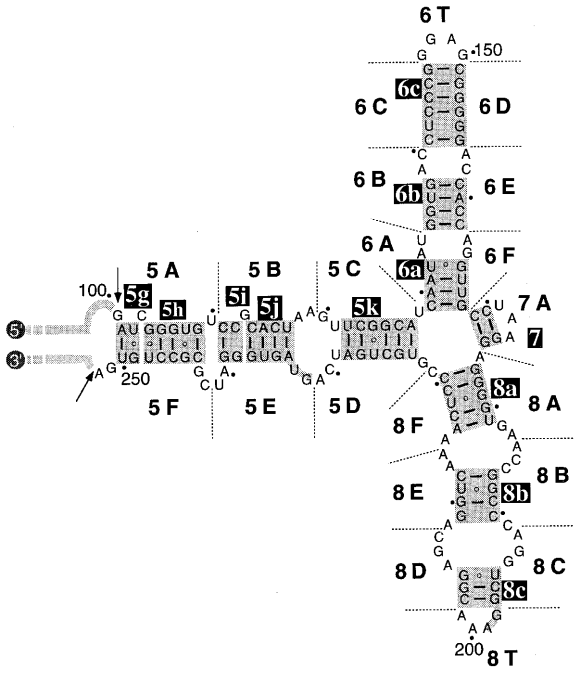

Figure 1. Location of mutations in the secondary structure of the large domain of human SRP RNA. Arrows indicate hypersensitive sites cleaved by micrococcal nuclease (31) which separate the large SRP domain from the rest of the particle (not shown). The 5′- and 3′-ends of the RNA molecule are labeled and helices are marked according to the nomenclature of (5). Residues are marked with dots in 10 nucleotide increments and by numbers in 50 nucleotide increments. Base pairings are highlighted in gray. Base paired sections of helices 5, 6 and 8 are given suffices g–k in helix 5, and a–c in helices 6 and 8. The borders between the helix-disrupting mutations (5A–F, 6A–F, 7A and 8A–F) and the two tetraloop mutations (6T and 8T) are indicated by the dotted lines. Additional information about each mutant can be found in Table 1.

cated previously (18). All mutations were confirmed by DNA sequencing using Sequenase (US Biochemicals).

T7 RNA polymerase was prepared as described (20) with modifications kindly provided by Arthur Zaug, University of Colorado, Boulder. DNAs of plasmids that carried the human SRP RNA or the mutant genes were restricted with *Dra*I, concentrated by phenol–chloroform extraction and ethanol precipitation, and were dissolved in 10 mM Tris–HCl, pH 7.5, 1 mM EDTA at a concentration of 1 µg/µl. Run-off transcriptions were carried out for 2 h at 37°C in 200 mM HEPES–KOH, pH 7.5, 30 mM $MgCl_2$, 2 mM spermidine, 40 mM DTT, 6 mM of each rNTP, 0.3–1 µg/µl of restricted DNA, and an amount of T7 RNA polymerase that was optimized empirically to maximize RNA yields. After transcription, 1/10 vol of 0.5 M EDTA, pH 8 and 0.4 vol of 9 M LiCl were added, the samples were incubated on ice for 30 min, and the RNAs were concentrated by centrifugation in a microfuge for 10 min. The pellets were washed with 1 ml of ice-cold 2.5 M LiCl, followed by centrifugation and a wash with 80% ethanol. The pellets were dried and the RNA was dissolved in a small volume of water and stored at –20°C. The RNA concentrations of the samples were determined by electrophoresis of appropriately diluted sample aliquots on 2% agarose gels followed by staining with ethidium bromide and calculated from a standard curve obtained with known amounts of *Escherichia coli* 5S rRNA (Boehringer) separated on the same gel.

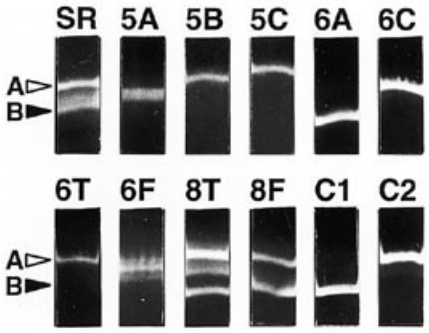

Figure 2. Separation of RNA conformers. Electrophoretic separation of unmutated SRP RNA (SR) and mutant derivatives 5A, 5B, 5C, 6A, 6C, 6T, 6F, 8T, 8F, C1 and C2 on 6% non-denaturing polyacrylamide gels. Mobilities of the slower migrating SRP RNA conformer SR-A (open arrow) and the faster migrating SR-B (filled arrow) are indicated.

Analysis of conformers

RNAs were incubated in 10 µl SRP reconstitution buffer (50 mM Tris–HCl pH 7.9, 300 mM KOAc, 5 mM $MgCl_2$, 1 mM DTT and 10% glycerol) at a concentration of 1 µg/µl at 60°C for 10 min followed by a gradual cooling to room temperature over ~30 min. The samples were incubated at 37°C for 6–10 min and were loaded (without addition of any tracking dye) onto a 6% polyacrylamide gel (acrylamide/bisacrylamide 40/0.8 w/w, 20 mM HEPES pH 8.3, 0.1 mM EDTA, 6% glycerol) which had been pre-electrophoresed at 15 mA for 30 min with 20 mM HEPES pH 8.3, 0.1 mM EDTA as a reservoir buffer (21). Control samples included *Hae*III-digested ϕX174 DNA to verify the linearity of the separation, and hSR and *E.coli* 5S rRNAs for confirming the ability of the gel to appropriately detect conformers. Electrophoresis at room temperature was continued at 15–20 mA until the bromophenol blue (loaded in a separate slot) had traveled for ~14 cm. The gel was stained for 10 min with 1 µg/ml ethidium bromide, and bands on the photographs of the ethidium bromide-stained gels were quantified with an Abaton 300/GS scanner and NIH Image software (22). The value ζ was determined using the formula:

$$\zeta = \frac{\sum_{i=2}^{n} i}{(n-1)i_1}$$

where n is the number of conformers and i_1 is the area under the largest peak.

Display of the large SRP RNA domain

The three-dimensional model of the human SRP RNA structure (11) was obtained from the SRP database (23) in the PDB file-format (24) at the Internet address http://pegasus.uthct.edu/SRPDB/SRPDB.html. The model was displayed on an Silicon Graphics Indigo 2 Extreme workstation using the program DRAWNA (25). The model was accepted as provided with no additional structural constraints. Experimental data were incorporated by color-coding mutated sections of the SRP RNA that had significant effects on the formation of the A or B-conformers as described in Results and Figure 4.

Table 1. Conformational effects in the mutant SRP RNAs

Name	Change	Expected effect on the SRP RNA	ζ	Form
hSR	None	None	0.73 ± 0.06	–
ΔH6	36 nt deleted (131–166)	Removes helix 6 from the SRP RNA	0	A[a]
ΔH67	48 nt deleted (128–175)	Removes helices 6 and 7	0	B[b]
ΔH8	48 nt deleted (175–222)	Removes helix 8	0	B[a]
5A	103-UCGGGUGU-110→GUCCGCG	Disrupts a segment of helix 5	ND	–
5B	111-CCGCACUAA-119→GGGUGAUG	Disrupts a segment of helix 5	0	A
5C	120-GUUCGGCAU-128→CCAGUCGUG	Disrupts a segment of helix 5	0	A
5D	222-GUGCUGAUCA-231→UACGGCUCGC	Disrupts a segment of helix 5	0.07 ± 0.01	A
5E	232-GUAGUGGGAU-241→AAUCACCCUC	Disrupts a segment of helix 5	0.20 ± 0.08	(B)
5F	242-CGCGCCUG-251→UUGUGGGU	Disrupts a segment of helix 5	0.52 ± 0.02	–
6A	129-CAAUAU-134→GUUGGA	Disrupts proximal segment of helix 6	0	B
6B	135-GGUGAC-140→CCACCA	Disrupts central segment of helix 6	0.22 ± 0.02	(A)
6C	141-CUCCCG-146→CGGGGG	Disrupts distal segment of helix 6	0	A
6T	147-GGAG-150→UUCG	Mutates tetraloop of helix 6	0	A
6D	151-CGGGGG-156→GCCCUC	Disrupts distal segment of helix 6	0.41 ± 0.06	–
6E	157-ACCACC-162→CAGUGG	Disrupts central segment of helix 6	0.50 ± 0.07	–
6F	163-AGGUUG-168→UAUAAC	Disrupts proximal segment of helix 6	0.39 ± 0.05	–
7A	169-CC-170→GG	Disrupts helix 7	0.07 ± 0.004	A
8A	176-AGGGGUGA-183→CCCUCAAG	Disrupts proximal segment of helix 8	0.43 ± 0.1	–
8B	184-ACCGGCCC-191→GAACUGGA	Disrupts central segment of helix 8	0.20 ± 0.06	(A)
8C	192-AGGUCG-197→CCAGGC	Disrupts distal segment of helix 8	0.32 ± 0.1	–
8T	198-GAAA-201→UUCG	Mutates tetraloop of helix 8	0.24 ± 0.05	(A)
8D	202-CGGAGC-207→GCUGCA	Disrupts distal segment of helix 8	0.14 ± 0.03	(B)
8E	208-AGGUCAA-214→CCCGGCC	Disrupts central segment of helix 8	0.26 ± 0.05	(B)
8F	215-AACUCCC-221→GUGGGGA	Disrupts proximal segment of helix 8	0.69 ± 0.3	–
C1	129-CAAUAU-134→GUUGGA	Compensates proximal segment of helix 6	0	B
	163-AGGUUG-168→UAUAAC			
C2	135-GGUGAC-140→CCACCA	Compensates central segment of helix 6	0.05 ± 0.01	A
	157-ACCACC-162→CAGUGG			
C3	141-CUCCCG-146→CGGGGG	Compensates distal segment of helix 6	0.03 ± 0.001	A
	151-CGGGGG-156→GCCCUC			

Mutants are listed in the left column; changes relative to unmutated human SRP RNA (hSR) with the expected effects on RNA structure are tabulated in the second and third columns and. ζ-values, indicating the degree of the conformational variability (see Materials and Methods), are shown in the fourth column. Data are compiled from at least three independent experiments with the standard error of the means shown. In the right column, the mobilities of dominant conformers ($0 \leq \zeta \leq 0.1$) relative to the A- or B-form of unmutated SRP RNA is indicated; for $0.1 < \zeta \leq 0.3$, the dominant conformer is listed in parentheses.
ND, not determined.
RNA of mutant 5A separated into two conformers of nearly identical mobility: [a]the mobilities of the large deletion mutants ΔH6 and ΔH8 relative to SR-A and SR-B were determined earlier (17); [b]RNAs from mutants ΔH67 and ΔH8 co-migrated on non-denaturing polyacrylamide gels (not shown) indicating that ΔH67 corresponds to the faster migrating B-form.

RESULTS

Systematic site-directed mutagenesis in the large SRP domain

The RNA secondary structure corresponding the large domain of the human SRP is shown in Figure 1 and includes a large portion of helix 5, as well as helices 6, 7 and 8. The majority of the mutations in this region were used earlier to characterize the binding sites of proteins SRP19 (18) and SRP54 (26). Alterations included a deletion of helix 6 (mutant ΔH6) or helix 8 (mutant ΔH8). PCR site-directed mutagenesis (18,19; and Materials and Methods) was used to construct mutant ΔH67, which lacks helices 6 and 7. The multiple residue changes of the other mutant RNAs were expected to disrupt base pairing in various helical sections as indicated in Figure 1 and listed in Table 1. There were

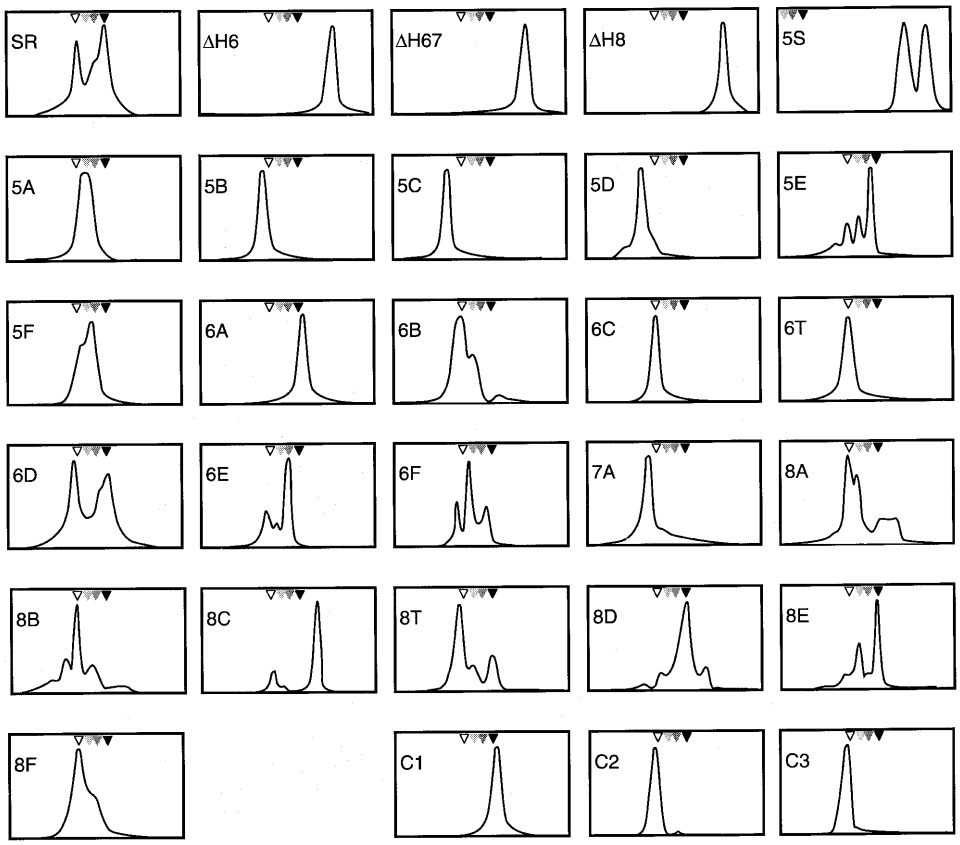

Figure 3. RNA conformer profiles. RNAs were separated on non-denaturing polyacrylamide gels as described in Materials and Methods. Photographs of the ethidium bromide-stained gels were scanned without applying enhancements and the profile of each lane was analyzed with the NIH Image program (22). Mobilities relative to the slower migrating conformer SR-A (▽) and the faster migrating SR-B (▼) are indicating on top of each panel. The gray triangles indicate the intermediate mobilities of two minor SRP RNA conformers (16).'5S' corresponds to *E.coli* 5S ribosomal RNA; all other designations are as shown in Table 1.

also three mutations in helix 6 that retained base pairing by changing both RNA strands in helix 6, and two tetranucleotide (tetraloop) mutants (6T and 8T). All RNAs were synthesized *in vitro* by run-off transcription with T7 RNA polymerase (Materials and Methods) using linearized derivatives of plasmid phSR as templates (14).

Analysis of SRP RNA conformers

RNAs were activated by incubation in SRP reconstitution buffer at 60°C followed by slow cooling to room temperature (Materials and Methods). For each mutant RNA, conformers were analyzed at room temperature by electrophoresis on native polyacrylamide gels. Human SRP RNA and *E.coli* 5S ribosomal RNA were used to confirm the appropriate separation of the conformers. After electrophoresis, the ethidium bromide-stained gels were photographed (Fig. 2) and profiles of the lanes were generated using Image software (22, Fig. 3). To quantitate the degree of conformational variability, a value ζ was calculated for each RNA (see Materials and Methods). (ζwas zero when a single conformer was identified, and had a theoretical value of one when there were two or more equally-represented conformers.) The two highest ζ-values were observed for *E.coli* 5S rRNA (0.80 ± 0.05) and the unmutated human SRP RNA (0.73 ± 0.06). All conformer profiles were highly reproducible as indicated by the low standard deviation of the means determined from at least three independent experiments (Table 1).

Nine mutant RNAs (ΔH6, ΔH67, ΔH8, 5B, 5C, 6A, 6C, 6T and C1) migrated as a single conformer (ζ = 0). Mutant 5A RNAs separated into two conformers of nearly identical mobility (Fig. 2). Minor conformational variability ($0 < \zeta \leq 0.1$) was detected in mutants 5D, 7A, C2 and C3, whereas mutants 5E, 6B, 8B, 8T, 8D and 8E had moderately low ζ-values between 0.1 and 0.3. Mutation 5F, as well as the three mutations of the 3′-portion of helix 6 (6D, 6E and 6F) and the three mutations 8A, 8C and 8F demonstrated considerable conformational variability ($\zeta > 0.3$) that in some cases approached the value obtained with the unmutated SRP RNA.

The majority of the mutations (exceptions were mutants 5E, 8D, 8E and the large helix deletion mutants ΔH6, ΔH67 and ΔH8) caused the formation of slowly-migrating A-forms. In contrast, only the two mutants 6A and C1 formed pure B-form RNAs. Since mutants 6A and C1 shared altered nucleotides at positions 129–134, changes of these residues appeared to be sufficient for inducing the B-conformation.

Figure 4. SRP RNA conformer-sensitivities in three dimensions. The relaxed stereoview of the large SRP domain was generated as described in Materials and Methods. Displayed are the folded backbone and the paired bases. SRP RNA helices 5–8 are labeled as such. The effects of the mutations on the formation of the two conformers are shown in red (SR-A) or green (SR-B) for pronounced effects ($0 \leq \zeta \leq 0.1$), and in orange (SR-A) and yellow (SR-B) for mild effects ($0.1 < \zeta \leq 0.3$). Regions of the RNA affected by the mutations with $\zeta > 0.3$ are coded in gray.

Localization of conformer-sensitive sites in 3D

To visualize better the effects of the mutations on SRP RNA conformation, we incorporated the results from the site-directed mutagenesis experiments into the current model of the three-dimensional structure of the SRP RNA (11). This hypothetical model is characterized by a relatively 'straight' helix 6 and by a 'bent' helix 8. Figure 4 shows a view of the large domain with color-coded regions in the RNA to highlight strong or mild influences on the formation of SR-A or SR-B. The calculated ζ-values were used to group the conformer behavior of each mutant RNA as described in the legend to Figure 4. Shown in red are those RNA regions that, when altered, favor A-like forms. Such sites were located throughout helices 5, 6 and 7, but were not found in helix 8. Only the 5′-proximal portion of helix 6, shown in green, constrained the RNA to a single B-conformer. Mild effects on SR-A or SR-B (shown in yellow and orange, respectively) were caused by mutations in the 3′-half of helix 6 and also by some sites in helix 8.

DISCUSSION

SRP RNA conformers

Reduced electrophoretic mobilities of nucleic acids on polyacrylamide gels reflect deviations from straight rods or from compact structures, as has been demonstrated in the study of nucleic acid bends (27,28). Furthermore, additional loops, bulges and branches can cause slower migration when compared to the mobility of a molecule with the same molecular weight that lacks these features (29,30). Thus, of the two conformers present in human SRP RNA, the faster migrating SR-B form is seen as a more compact and/or less flexible molecule when compared to the slow-moving A-form (17,29).

Our results show that the majority of nucleotide changes cause a shift to A-like conformers. This is to be expected as additional internal loops are introduced by the disruption of helical sections. The same effect may be caused by mutations that disrupt the three-dimensional structure of a tightly folded SRP RNA. For example, mutants 5B, 5C and 5D behave similarly to SR-A, but their mobilities are progressively reduced even further as the mutations approach the junction of the various RNA helices. Other slight deviations from the mobilities of SR-A and SR-B are interpreted as minor perturbations of the RNA structure, possibly combined with changes in molecular weight. A small percentage of RNA molecules with conformations that deviate considerably from pure A- and B-forms are seen in some mutant RNAs and in the unmutated SRP RNA (Figs 2 and 3). These molecules could be the result of an incomplete renaturation process or might represent distinct intermediate steps that occurred during the conversion between the prevalent SR-A and SR-B forms.

When we tested the influence of monovalent (K^+ at 0, 50, 300 or 500 mM) and divalent cations (Mg^{2+} at 0, 5, 10 or 30 mM), the A-form was a prominent component within this wide range of experimental conditions. This indicated that SR-A was not simply an artifact that was generated during the chosen SRP reconstitution conditions (300 mM KOAc, 5 mM $MgCl_2$). Both SR-A and SR-B formed independently of heating to 60°C and slow-cooling (data not shown). However, we performed this step because activation and renaturation are considered to be necessary for melting possible trapped intermediates that might have formed during sample preparation.

Assembly of SRP19 and SRP54 the large SRP domain

We consider it significant that out of the 149 residues altered, only six induced the single B-form. Protein SRP19 is the primary assembly protein of the SRP and binds alongside the 5′-portion of helix 6 (18). The affinity of protein SRP19 to the more compact B-conformer was ~3.5 times greater than to the looser A-conformer (17). Since the sequence 129-CAAUAU-134 (Fig. 4) is located within the SRP19 binding site, we propose that it is a trigger site which is activated upon SRP19 binding to helix 6. This view is consistent with the idea that the tetraloop of helix 6 serves as a nucleation site in SRP assembly (26), and that the region at the proximal portion of helix 6, when touched by SRP19, triggers the formation of SR-B. Nevertheless, we do not exclude the possibility that conformational switching may occur in the fully-assembled SRP (8).

In mammals, protein SRP54 interacts with the SRP RNA only after an SRP19–RNA complex has been formed (10). However, induction of SR-B by SRP19 is insufficient for the association with SRP54. As we have shown recently (26), the M-domain of human SRP54 (SRP54M) will not interact with a mixture of SRP RNA molecules that contains a substantial amount of SR-B. Furthermore, when SRP19 was absent, neither the pure B-form mutant 6A nor C1 bound even trace amounts of SRP54M. Thus, after the induction of the SR-B conformer, additional structural changes may occur in the RNA or in the protein during the organization of the SRP19–RNA complex. Furthermore, since SRP19 is an integrated part of the SRP, protein–protein interactions between RNA-bound SRP19 and protein SRP54 may be required to complete the assembly.

ACKNOWLEDGEMENTS

We thank Shaun D. Black for critical reading of the manuscript. This work was supported by NIH grant GM-49034 to C.Z.

REFERENCES

1 Cech, T., Zaug, A., and Grabowski, P. (1981) *Cell*, **27**, 487–496.
2 Guerrier-Takada, C., Gardiner, K., Marsh, T., Pace, N., and Altman, S. (1983) *Cell*, **35**, 849–857.
3 Noller, H., Hoffarth, V., and Zimniack, L. (1992) *Science*, **256**, 1416–1419.
4 Lütcke, H. (1995) *Eur. J. Biochem.*, **228**, 531–550.
5 Larsen, N., and Zwieb, C. (1991) *Nucleic Acids Res.*, **19**, 209–215.
6 Andrews, D., Walter, P., and Ottensmeyer, P. (1987) *EMBO J.*, **6**, 3471–3477.
7 Siegel, V., and Walter, P. (1988) *Proc. Natl. Acad. Sci. USA*, **85**, 1801–1805.
8 Andreazzoli, M., and Gerbi, S. A. (1991) *EMBO J.*, **10**, 767–77.
9 Gundelfinger, E. D., DiCarlo, M., Zopf, D., and Melli, M. (1984) *EMBO J.*, **3**, 2325–2332.
10 Walter, P., and Blobel, G. (1983) *Cell*, **34**, 525–533.
11 Zwieb, C., Müller, F., and Larsen, N. (1996) *Folding Des.*, **1**, 315–324.
12 Lütcke, H., Prehn, S., Ashford, A., Remus, M., Frank, R., and Dobberstein, B. (1993) *J. Cell Biol.*, **121**, 977–985.
13 Lingelbach, K., Zwieb, C., Webb, J. R., Marshallsay, C., Hoben, P. J., Walter, P., and Dobberstein, B. (1988) *Nucleic Acids Res.*, **16**, 9431–9442.
14 Zwieb, C. (1991) *Nucleic Acids Res.*, **19**, 2955–2960.
15 Zwieb, C. (1985) *Nucleic Acids Res.*, **13**, 6105–6124.
16 Zwieb, C., and Ullu, E. (1986) *Nucleic Acids Res.*, **14**, 4639–4657.
17 Walker, P., Black, S., and Zwieb, C. (1995) *Biochemistry*, **34**, 11989–11997.
18 Zwieb, C. (1992) *J. Biol. Chem.*, **267**, 15650–15656.
19 Nelson, R. M., and Long, G. L. (1989) *Anal. Biochem.*, **180**, 147–151.
20 Butler, E., and Chamberlin, M. (1982) *J. Biol. Chem.*, **257**, 5772–5778.
21 Wolffe, A. (1988) *EMBO J.*, **7**, 1071–1079.
22 Rasband, W. (1994) The Image program is in the public domain and available by Anonymous FTP from zippy.nimh.nih.gov.
23 Larsen, N., and Zwieb, C. (1996) *Nucleic Acids Res.*, **24**, 80–81.
24 Bernstein, F., Koetzle, T., Williams, G., Meyer, E., Jr, Brice, M., Rodgers, J., Kennard, O., Shimanouchi, T., and Tasumi, M. (1977) *J. Mol. Biol.*, **112**, 535–542.
25 Massire, C., Gaspin, C., and Westhof, E. (1994) *J. Mol. Graphics*, **12**, 201–206.
26 Gowda, K., Chittenden, K., and Zwieb, C. (1997) *Nucleic Acids Res.*, **25**, 388–394.
27 Wu, H., and Crothers, D. (1986) *Nature*, **308**, 509–513.
28 Zwieb, C., Kim, J., and Adhya, S. (1989) *Genes Dev.*, **3**, 606–611.
29 Gast, F., and Hagerman, P. (1991) *Biochemistry*, **30**, 4268–4277.
30 Tang, R., and Draper, D. (1994) *Biochemistry*, **33**, 10089–10093.
31 Gundelfinger, E. D., Krause, E., Melli, M., and Dobberstein, B. (1983) *Nucleic Acids Res.*, **11**, 7363–7374